



Published in final edited form as:

*Ann Biomed Eng.* 2013 December ; 41(12): . doi:10.1007/s10439-013-0872-9.

## Tubular Heart Valves from Decellularized Engineered Tissue

**Zeeshan H. Syedain, Ph.D.<sup>1,\*</sup>, Lee A. Meier, B.Bm.E., B.S.<sup>1,\*</sup>, Jay Reimer, B.S.<sup>1</sup>, and Robert T. Tranquillo, Ph.D.<sup>1,2</sup>**

<sup>1</sup>Department of Biomedical Engineering, University of Minnesota

<sup>2</sup>Department of Chemical Engineering & Materials Science, University of Minnesota

### Abstract

A novel tissue-engineered heart valve (TEHV) was fabricated from a decellularized tissue tube mounted on a frame with three struts, which upon back-pressure cause the tube to collapse into three coapting “leaflets”. The tissue was completely biological, fabricated from ovine fibroblasts dispersed within a fibrin gel, compacted into a circumferentially-aligned tube on a mandrel, and matured using a bioreactor system that applied cyclic distension. Following decellularization, the resulting tissue possessed tensile mechanical properties, mechanical anisotropy, and collagen content that were comparable to native pulmonary valve leaflets. When mounted on a custom frame and tested within a pulse duplicator system, the tubular TEHV displayed excellent function under both aortic and pulmonary conditions, with minimal regurgitant fractions and transvalvular pressure gradients at peak systole, as well as effective orifice areas exceeding those of current commercially available valve replacements. Short-term fatigue tests of one million cycles with pulmonary pressure gradients was conducted without significant change in mechanical properties and no observable macroscopic tissue deterioration. This study presents an attractive potential alternative to current tissue valve replacements due to its avoidance of chemical fixation and utilization of a tissue conducive to recellularization by host cell infiltration.

### Keywords

Heart Valve; Tissue Engineering; Pulse Duplicator; Decellularization

## 1. Introduction

The concept of tissue engineering a heart valve was proposed over 15 years ago, first as leaflets<sup>1</sup> and then as complete valves<sup>2</sup>. Since then, several groups have developed various strategies to develop a tissue-engineered heart valve (TEHV), with considerable testing in animal models performed already<sup>3–8</sup>. The pediatric patient population would most clearly benefit from a TEHV to replace the pulmonary valve (PV), the valve most frequently indicated with congenital defects, thereby obviating the need for multiple placements with a larger prosthetic valve as the child grows. However, a TEHV that could replace the aortic valve (AV) in adults would, in theory, preclude the necessity for life-long anticoagulation therapy needed for mechanical valves, or the prospect of a replacement tissue valve due to its eventual failure from calcification. Unlike a pediatric TEHV, an adult TEHV, such as the one proposed herein, can involve inert materials.

Corresponding author: Robert T. Tranquillo, Department of Biomedical Engineering, 7-114 NHH, 312 Church St SE, University of Minnesota, Minneapolis, MN 55455, Tel: 612-625-6868, Fax: 612-626-6583, tranquillo@umn.edu.

\*Co-first Authors

In the vast majority of the animal studies the implanted TEHV has ultimately failed, with a common failure mode being leaflet retraction (shortening) and/or thickening. The progressive contraction of the tissue by the transplanted cells, the cells used to fabricate the tissue *in vitro*, has been implicated in several of these studies<sup>7,8</sup>. One remedy for this problem may be decellularizing the tissue prior to implantation<sup>9,10</sup>. It has been shown that decellularized small-diameter tissue tubes implanted as arterial grafts undergo relatively rapid (within 1–2 months), extensive recellularization<sup>11,12</sup> and favorable remodeling of the extracellular matrix, including elastin deposition within 6 months **without any evidence of dilatation or mineralization**<sup>12</sup>. Decellularization prior to implantation enables constructs to be fabricated using allogeneic cell sources as removal of cellular material renders the tissue non-immunogenic<sup>11,12</sup>. Furthermore, decellularization also allows for long-term storage of the engineered tissues without any appreciable loss of mechanical properties<sup>11,12</sup>. In this way, tissue fabrication can be moved off-line. The ability to engineer non-immunogenic tissues from human cells that can be stored and are thus available to patients “off-the-shelf” is an exceedingly attractive prospect.

All TEHV designs to date have been based on the creation of leaflets, either attached to a tube<sup>2,13</sup> or created so as to be contiguous with the tube as it formed<sup>14–16</sup>. This is obviously motivated by the design of semi-lunar valves such as the PV and AV. However, there are several commercial bioprosthetic valves that are based on the concept of valve action created by diastolic backpressure causing the inward collapse of a tube that is constrained at three points along the periphery. For example, a design incorporating the use of three sutured anchor points to form the equivalent of three coapting leaflets between the points of constraint was first proposed by Cox *et al*<sup>17</sup>. Current tissue-based valves commonly employ pieces of xenogeneic pericardium sewn into a tube and placed around the frame. In some cases tabs are placed at the three commissures in order to allow for suturing of the valve to the existing root so as to provide the needed constraints without the use of a frame.

Despite the relative success of engineered small-diameter tissue tubes as arterial grafts, engineering a large diameter tissue tube for use as a TEHV based on the collapsing tubular heart valve design has not been reported. In this study, we fabricated 22 mm internal diameter (ID) tissue by entrapping ovine dermal fibroblasts (oDFs) in a tubular fibrin gel and mechanically constraining the cell-induced gel compaction with a mandrel to achieve circumferential fiber alignment<sup>18</sup> (ovine cells were used in prelude to a preclinical study). This was followed by conditioning in a pulsed flow-stretch bioreactor to stimulate collagen production and achieve physiological mechanical and functional properties<sup>19</sup>. We then characterized their function as a tubular TEHV in a pulse duplicator system. The tissue tubes were first decellularized and then mounted on a frame presenting three struts machined from poly-etheretherketone (PEEK). The tubular TEHVs were evaluated under pulmonary and aortic flow conditions in a custom pulse duplicator system, and short-term (1M and 2M cycle) durability tests were performed on two valves. They were also subjected to mechanical, compositional, and histological characterization and analyses.

## 2. Materials and Methods

### 2.1. Engineered tissue tubes

Ovine dermal fibroblast (oDF)-seeded fibrin gel was formed by adding thrombin (Sigma) and calcium chloride in 20 mM HEPES-buffered saline to a suspension of oDF (Coriell, from one donor) in bovine fibrinogen (Sigma, F8630). The final component concentrations of the cell suspension were as follows: 4mg/ml fibrinogen, 0.38U/ml thrombin, 5.0 mM Ca<sup>++</sup>, and 1 million cells/ml. Cell suspensions were mixed and injected into a tubular glass mold with a 22 mm ID mandrel pre-treated with a solution of 5% Pluronic F-127 (Sigma, P2443) in distilled water. A Dacron<sup>®</sup> cuff was embedded on each end of the gel to facilitate

handling. Following gelation, the tubes were cultured in DMEM supplemented with 10% fetal bovine serum (FBS, HyClone), 100U/ml penicillin, 100µg/ml streptomycin, 0.25µg/ml amphotericin B (Gibco), 2µg/ml insulin (Sigma), 50µg/ml ascorbic acid (Sigma). After an initial 2-week maturation period, the tubes were transferred to a custom pulsed-flow-stretch bioreactor for an additional 3-week maturation period as previously described<sup>19</sup>. The flow-stretch bioreactor employed for these studies included a modification from previous designs<sup>20,21</sup>; the tubes were first mounted on a segment of latex tubing to provide an inner support in order to prevent fibroblast-mediated tissue necking and contraction during bioreactor maturation. The final dimensions of each engineered tissue tube were ~4 cm in length, 22 mm inner diameter, and ~800 µm in thickness.

For decellularization, the tubes were rinsed in phosphate-buffered saline (PBS) and incubated on an orbital shaker at room temperature for 6 hr with 1% sodium dodecyl sulfate (SDS, Sigma) in distilled water. The SDS solution was changed three times: at 30 minutes, 1 hour, and 4 hours. The tubes were rinsed in PBS and incubated at room temperature with 1% Triton X-100 (Sigma) in distilled water for 30 min, extensively washed with PBS for 72 hr, and then incubated in 2U/ml deoxyribonuclease (Worthington Biochemical, DR1) in DMEM supplemented with 10% FBS for 4 hours.

## 2.2. Valve design

The decellularized 22 mm ID engineered tissue tube was mounted onto a custom frame machined from PEEK. The frame had an **outer** diameter of 19 mm with a wall thickness of 1.5 mm. The crown of the frame had a height of 16 mm. The engineered tissue tube was cut to ~20 mm length, slightly longer than the frame height, and secured to the frame using interrupted 4-0 prolene sutures. The larger diameter tissue tube compared to the frame diameter (22 mm vs. 19 mm) was utilized to allow for full coaptation of the valve during diastole.

## 2.3. Pulse duplicator testing

A customized pulse duplicator system was designed based on a commercial wave generator and pump (ViVitro Systems). The system is shown in Figure 1. The custom pulse duplicator loop consists of a reservoir, valve mounting chamber, variable compliance chamber, and mechanical bi-leaflet valve to ensure one-directional fluid movement. The system has pressure transducers (ViVitro Systems) immediately above and below the valve to allow for accurate pressure measurements. Additionally, there is an electromagnetic flow meter (Carolina Medical, 500 series flowmeter) upstream of the valve to measure the flow rate in both directions. A custom LabVIEW<sup>®</sup> program was used to record flow rates and pressures. For testing, the tubular TEHV was mounted in the valve chamber by press-fitting into a custom-molded silicone rubber tube. The silicone rubber tube ensures no paravalvular leakage during the testing. The pulse duplicator loop was run with PBS with 100U/ml penicillin, 100µg/ml streptomycin added. Each valve was tested with pressure conditions to mimic PV (30 over 20mmHg with diastolic transvalvular pressure of 11±3 mmHg) and AV (120 over 80mmHg with diastolic transvalvular pressure of 100±15 mmHg) pressure conditions. Pressure was controlled by changing the downstream flow resistance, stroke volume, and upstream hydraulic pressure head.

During valve testing, end-on camera (Canon EOS T3i) images were obtained at 60fps for video capture. Images extracted from the video were imported into ImageJ<sup>®</sup> software to measure the open area of the valve during systole to report the effective orifice area (EOA).

Additionally, valves were conditioned at 120 cycles/min for ~1 million (n=1) and ~2 million (n=1) cycles at pulmonary pressure gradients. The fatigue-tested valves were visually

inspected for deterioration. Additionally, their mechanical properties were measured and compared to a non-fatigued sample.

#### 2.4. Mechanical testing

Tissue strips cut from the engineered tissue tube and ovine pulmonary valve leaflets of dimension  $\sim 2 \text{ mm} \times 10 \text{ mm}$  were tested for tensile properties in both the circumferential and radial directions with respect to the valve “leaflets” (for the tubular valve, the circumferential and radial directions of the “leaflets” are the circumferential and axial directions of the tube, respectively). Thickness was measured using a digital caliper. Tissue strips were placed in compressive grips, attached to the actuator arm and load cell of an InstronMicroBionix (Instron Systems), and straightened with an applied load of 0.005 N. This position was used as the reference length of the strip. Following 6 cycles of 0–10% strain conditioning at 2 mm/min, strips were stretched to failure at the same rate. True strain was calculated based on the natural log of the tissue length divided by the reference length. The stress was calculated as force divided by the initial cross-sectional area. The tangent modulus (E) was determined as the slope of the linear region of the stress-strain curve prior to failure. The peak stress was defined as ultimate tensile strength (UTS). Mechanical anisotropy was defined as the ratio of the modulus of tissue samples cut in the circumferential direction to the modulus of samples cut from the tissue in the axial direction.

#### 2.5. Tissue composition and DNA analysis

The collagen mass content was quantified using a hydroxyproline assay previously described<sup>22</sup> assuming 7.46 mg of collagen per 1 mg of hydroxyproline. The total protein content was measured using the ninhydrin assay<sup>23</sup>. The tissue sample volume was calculated using the measured length, width, and thickness of the strips (as described above for uniaxial testing). Collagen and protein concentrations were calculated as mass per unit volume. The cell content was quantified with a modified Hoechst assay for DNA assuming 7.7 pg of DNA per cell<sup>24</sup>. Cell concentration was calculated as the number of cells per unit volume.

#### 2.6. Histology and polarized light imaging

Circumferential tissue strips were fixed in 4% paraformaldehyde, embedded in OCT (Tissue-Tek), and frozen in liquid N<sub>2</sub>. Cross sections of 9- $\mu\text{m}$  thickness were stained with Lillie’s trichrome and picosirius red stains. Images were taken at 10 $\times$  magnification using a color CCD camera. For picosirius red staining, images were taken with the sections placed between crossed-plane polarizers. Fiber alignment was measured using a polarized light imaging method as described previously<sup>25</sup>.

#### 2.7. Statistics

For all experiments **besides fatigue testing**,  $n=3$  or higher sample number was used. For fatigue testing, measurements from each “leaflet” on a single sample were taken and compared to the same tissue that was not subjected to fatigue testing. Statistical significance of differences between **two** groups was determined using Student’s t-test. Any reference to a difference in the Results and Discussion sections implies statistical significance at the level  $p < 0.05$ .

### 3. Results

#### 3.1. Tubular TEHV design and development

The tubular TEHV was created by mounting a decellularized engineered tissue tube onto a PEEK frame (Fig. 2). The engineered tissue was tested for tensile mechanical properties after decellularization. The properties of the engineered tissue along with the ovine

pulmonary valve leaflet properties are shown in Table 1. The engineered tissue was approximately twice as thick compared to native leaflets; however, no statistical difference existed in the UTS or Modulus. The engineered tissue also displayed a mechanical anisotropy comparable to the native leaflet (**stress-strain curves shown in Fig. 3**). The tissue tube mounted onto a frame was also imaged for alignment (Fig. 4a). The polarized light imaging showed a strong circumferential fiber alignment (Fig. 4b), consistent with the mechanical anisotropy. The collagen and protein concentrations of the engineered tissue were also comparable to that of the native leaflets. The DNA content was reduced by  $97\pm 1\%$  during the decellularization process for the engineered tissue.

### 3.2. Pulse duplicator testing

Tubular TEHVs ( $n=3$ ) were tested in the pulse duplicator loop at pulmonary and aortic conditions. The values of key performance metrics are reported in Table 2. For both pulmonary and aortic conditions, an average flow rate of 5 LPM was used. Figure 5 shows representative flow rate and pressure profiles for each condition. There was a “water hammer” effect evident during valve closure, which accounts for the negative ventricular pressure observed immediately after valve closure and its subsequent fluctuation. The pressures recorded up-stream and down-stream of the valve (blue and red lines) were averaged over 3 cycles when the valve was completely open to report the systolic pressure drop and when the valve was completely closed to report the diastolic pressure drop. Both systolic and diastolic pressure drop values were different between pulmonary and aortic conditions. The EOA was comparable for both pressure conditions. Representative images of the tubular TEHV during a cardiac cycle are shown in Figure 6. The regurgitation volume (taken as the ratio of negative volume to total cycle volume) was comparable between pulmonary and aortic conditions, and only occurred during the closing phase of the cycle. During the end diastolic phase, negative flow rate was not observed, indicating no leakage when the tubular TEHV was fully closed.

### 3.3. Histological evaluation

Decellularized engineered tissue tubes were fixed and stained using Lillie’s trichrome and picrosirius red. Figure 7a shows a representative trichrome image of the tissue, with cell-produced collagen in green and residual fibrin in red. Fibrin was observed near the luminal surface of the tissue, which was in contact with the impermeable mandrel during static culture. Consistent with the quantification of the residual DNA within the constructs, Lillie’s trichrome staining indicated the vast majority of cellular material was removed. Figure 7b shows the picrosirius red staining imaged under polarized light, with robust red staining of organized and circumferentially-aligned collagen fibers. The fiber alignment observed under polarized light imaging was consistent with the measured mechanical anisotropy.

### 3.4. Cyclic testing of the tubular TEHV over 1 and 2 million cycles

One tubular TEHV was fatigue tested under pulmonary pressure conditions (average 8mmHg end-diastolic pressure drop) at accelerated 120 cycles/min for a total of 1,036,800 cycles. After harvest, the valve was visually inspected for tears near its edges and near the suture locations. No macroscopic tissue damage was evident (Fig. 8a&b). The fatigued valve tissue had thickness of  $0.70\pm 0.05$ mm compared with  $0.80\pm 0.04$  mm for control tissue. The UTS ( $1.9\pm 0.3$  MPa) and modulus ( $3.2\pm 0.6$  MPa) of the fatigued tissue were not different from the non-fatigued tissue (Table 1) indicating no change in mechanical properties over 1 million cycles. A tubular TEHV from a second set of engineered tissue tubes was subjected to the same fatigue test, along with periodic UV light treatment of the medium reservoir to ensure sterility, for approximately two million cycles. Again, there was no evidence of altered valve function or gross tissue changes, except for some thinning of tissue in contact

with the three frame struts. The region from behind the strut was also sectioned into a circumferential strip and mechanically tested. Its thickness was one-half the “leaflet” thickness ( $0.39\pm 0.02\ \mu\text{m}$  vs.  $0.78\pm 0.04\ \mu\text{m}$ ) and exhibited approximately the same break force ( $4.6\pm 0.44\ \text{N}$  vs.  $4.2\pm 0.37\ \text{N}$ ). The functionally relevant failure tension (break force normalized to length) was thus no different ( $1680\pm 175\ \text{N/m}$  vs.  $1760\pm 16\ \text{N/m}$ ) although the thinner tissue contacting the strut possessed approximately twice the UTS ( $4.4\pm 0.70\ \text{MPa}$  vs.  $2.3\pm 0.12\ \text{kPa}$ ).

#### 4. Discussion

Herein we describe a novel tubular TEHV design, where a decellularized engineered tissue tube is mounted on a frame with three struts to create tri-leaflet valve function. This design circumvents the challenges associated with tri-leaflet valve fabrication using complex 3D molds<sup>16,26</sup> and joining leaflets to a root. It also leverages the commercial success of the tubular valve design, which uses chemically cross-linked xenogeneic pericardium sutured into a tube<sup>17</sup>.

Following *in vitro* culture and decellularization, the engineered tissue tube displays tensile mechanical properties and anisotropy similar to native PV tissue. The UTS and modulus of the engineered tube tissue were not different from values for ovine pulmonary valve leaflets. The mechanical anisotropy was primarily due to alignment of collagen fibers as seen with polarized light imaging of bulk fibers and picosirius red staining of collagen fibers. While substantial variability is present in the literature data on heart valve mechanical properties across different species, the decellularized engineered tissue has tensile strength comparable to human AV and PV leaflets<sup>27</sup>. In addition, the collagen concentration of the engineered tissue is 76% of native valve tissue, however the difference was not statistically different.

Lillie’s trichrome staining indicated substantial residual compacted fibrin near the luminal surface of the tissue tubes employed in these studies. It is hypothesized that this is a result of the impermeant luminal supports used during both static and bioreactor maturation (glass and latex, respectively) and the nutrient gradients that result across the tissue thickness due to a lack of luminal culture medium contact. It would be desirable in future studies, and for *in vivo* evaluation, to employ a tissue displaying homogenous remodeling throughout the tube thickness. This could likely be achieved through enhanced nutrient transport during bioreactor maturation via microporation of the latex support tubing in order to enable transmural nutrient delivery originating from the luminal surface.

To date, TEHVs made from a variety of biodegradable polymers and cell types have been evaluated as pulmonary valve replacements in the sheep model. More recently, implant studies have also been performed using a primate model<sup>28</sup>. While the data provide valuable insights regarding the important considerations to take into account for the development of tissue engineered heart valves, most studies have failed to show long-term durability and adequate function. One common failure mode has been associated with progressive leaflet shortening resulting from the contractile nature of the transplanted cells<sup>7,8</sup>. In order to address this, removal of the contractile cells prior to implantation by decellularization has been proposed as a viable solution with both biological and synthetic polymer-based tissue engineered valves. This approach also presents the potential for recellularization of the leaflets or valve conduit prior to implantation with non-contractile, matrix-producing cells<sup>9,10</sup>. For this reason, and the prospects of vastly increased commercializability and clinical utility, decellularized, engineered tissue tubes were used in these studies. While several cell sources provide a viable option for creating engineered tissue, extensive work in our lab<sup>10,19,29–31</sup> has shown the dermal fibroblast to be a promising option with the advantage of being a readily available source. In current experiments, 3% of the DNA

remained after decellularization as quantified with the Hoechst assay. Additional treatment with deoxyribonuclease could reduce residual DNA further. It remains to be seen even if a 3% residual will induce a significant immune reaction. In allogeneic decellularized implants possessing 14% residual DNA, no immune reaction was reported<sup>33</sup>.

The tubular TEHV was tested in a pulse duplicator system for hydrodynamic performance of the valve under both pulmonary and aortic conditions. Two critical metrics during the systolic phase are pressure drop across the valve and effective orifice area. There is a paucity of reported data for pulse duplicator testing of TEHVs. Therefore, reported data for commercial bioprosthetic valves made from porcine AV leaflets and bovine pericardium were used for comparison. For the tubular TEHVs, the values shown in Table 2 are comparable, if not superior, to reported data. For example, a commercial valve made from fixed bovine pericardium with 19 mm diameter displayed a systolic pressure drop of 10–16 mmHg and EOA of 1.4–1.5 cm<sup>2</sup> (53%, based on a 19 mm circle)<sup>17</sup>. For valves fabricated from porcine leaflets, the reported values are 25 mmHg and 1.1 cm<sup>2</sup>, respectively<sup>34</sup>. A likely reason for the low pressure drop and large EOA seen with the tubular TEHV is the physiological stiffness of the (non-fixed) engineered tissue used here; all commercially-available bioprosthetic valves undergo chemical fixation to eliminate tissue immunogenicity, which significantly increases their stiffness<sup>35–37</sup>.

Optimization of the frame design and method for mounting the tissue therein plays a critical role in the hydrodynamic properties of the valve's function, specifically, minimization of reverse flow and backpressure needed for prompt valve closure. For the tubular TEHV, the regurgitant fraction was approximately 5% under both aortic and pulmonary conditions, a value that is comparable to most commercially-available bioprosthetic valves<sup>34</sup>. The comparable regurgitant fraction indicates that the tubular TEHV exhibits a normal closure time. Based on the lack of reverse flow during the diastolic phase of the cycle, it can also be concluded that when the tubular TEHV is completely closed, there is no regurgitation, indicating an acceptable seal of the engineered tissue tube around the PEEK frame.

The ultimate goal for the tubular TEHV is recellularization *in vivo* and for the invaded host cells to then remodel the engineered tissue and regulate its repair and homeostasis indefinitely. Implantation of similarly fabricated 4 mm diameter engineered tissue tubes as femoral grafts into sheep revealed extensive recellularization after 2 months without a change in mid-graft diameter<sup>12</sup>. Therefore, fatigue testing of the tubular TEHV for much longer times, as is done for bioprosthetic heart valves, is not relevant. Preliminary fatigue testing at pulmonary conditions corresponding to 2 weeks duration *in vivo* (one million cycles) showed neither change in the mechanical properties of the tubular TEHV nor evidence of tissue degeneration. After the equivalent of 4 weeks (two million cycles), there was evidence of tissue thinning where contacting the three frame struts. The mechanical testing data of this thinned tissue (similar break force, twice the UTS) suggests the thinning was thus likely due to compression between the PEEK frame and the outer wall of the pulse duplicator system and not due to fatigue induced degeneration. This suggests that the non-fixed tissue can be implanted and sustained for the weeks prior to extensive recellularization expected *in vivo*, but that eventual recellularization will be crucial to maintenance of the collagenous matrix. Whether and how recellularization occurs in the "leaflets" (e.g., from cells derived from the host tissue or blood), which have no analogue in the femoral grafts made from similarly prepared decellularized tissue that exhibited extensive recellularization after two months without a change in mid-graft diameter<sup>12</sup>, will require implantation studies.

Historically, the ovine model has been employed in the preclinical evaluation of heart valve replacements. In preparation for implantation of the valve design described herein, ovine dermal fibroblasts were used for tissue fabrication in order to delineate the *in vivo* function

of these valves using decellularized, allogeneic tissue in the absence of immunosuppressive therapy. Ultimately, the insights gained from such studies would be used to guide development of an analogous therapy using human cells in order to translate these studies to a clinical setting.

Overall, testing of the tubular TEHV indicates its potential as a PV or AV replacement. If the “leaflets” of these mounted 22 mm ID engineered tissue tubes show recellularization *in vivo*, as has been observed for the same tubes made in 4 mm ID size for allogeneic femoral grafts in sheep<sup>12</sup>, without tissue retraction and with maintenance of valvular function in animal studies, the present design may be suitable for adult valve replacement. Future designs could possibly incorporate a biodegradable plastic frame or a tissue tube sewn directly into the orthotopic valve position. These two alternative approaches might enable the TEHV to grow with the patient, which is desired for pediatric valve replacements.

## 5. Conclusions

The data presented here describe the ability to utilize a decellularized engineered tissue tube obtained from mechanically-constrained fibrin gel compaction and remodeling by allogeneic dermal fibroblasts, for function as a TEHV. The decellularized engineered tissue tubes display compositional and mechanical properties similar to those observed in native ovine heart valve tissue, including a high degree of mechanical anisotropy that is characteristic of the aortic root and valve leaflets. Hydrodynamic performance of the tubular TEHV in a pulse duplicator system was comparable to commercial bioprosthetic valves, with a small transvalvular pressure gradient and regurgitant fraction, as well as an effective orifice area approaching unity. Durability of the tubular TEHV for the time expected for substantial recellularization *in vivo* (4 weeks) was demonstrated. This study demonstrates the feasibility of generating a functional TEHV by mounting a decellularized engineered tissue tube onto a custom frame.

## Acknowledgments

Authors will like to thank Naomi Ferguson, and Jillian Schmidt for technical assistance and Dave Hultman Design for machining the custom pulse duplicator system, bioreactor manifold and valve frames. The funding for the work was provided by NIH R01 HL107572 (to RTT).

## References

1. Shinoka T, Breuer CK, Tanel RE, Zund G, Miura T, Ma PX, Langer R, Vacanti JP, Mayer JE Jr. Tissue engineering heart valves: valve leaflet replacement study in a lamb model. *Ann. Thorac. Surg.* 1995; 60:S513–S516. [PubMed: 8604922]
2. Hoerstrup SP, Sodian R, Daebritz S, Wang J, Bacha EA, Martin DP, Moran AM, Guleserian KJ, Sperling JS, Kaushal S, Vacanti JP, Schoen FJ, Mayer JE Jr. Functional living trileaflet heart valves grown *in vitro*. *Circulation.* 2000; 102:III44–III49. [PubMed: 11082361]
3. Sodian R, Hoerstrup SP, Sperling JS, Daebritz S, Martin DP, Moran AM, Kim BS, Schoen FJ, Vacanti JP, Mayer JE Jr. Early *in vivo* experience with tissue-engineered trileaflet heart valves. *Circulation.* 2000; 102:III22–III29. [PubMed: 11082357]
4. Schmidt D, Dijkman PE, Driessen-Mol A, Stenger R, Mariani C, Puolakka A, Rissanen M, Deichmann T, Odermatt B, Weber B, Emmert MY, Zund G, Baaijens FP, Hoerstrup SP. Minimally-invasive implantation of living tissue engineered heart valves: a comprehensive approach from autologous vascular cells to stem cells. *J. Am. Coll. Cardiol.* 2010; 56:510–520. [PubMed: 20670763]
5. Emmert MY, Weber B, Behr L, Frauenfelder T, Brokopp CE, Grunenfelder J, Falk V, Hoerstrup SP. Transapical aortic implantation of autologous marrow stromal cell-based tissue-engineered heart



- valves: first experiences in the systemic circulation. *JACC. Cardiovascular interventions*. 2011; 4:822–823. [PubMed: 21777893]
6. Dijkman PE, Driessen-Mol A, de Heer LM, Kluin J, van Herwerden LA, Odermatt B, Baaijens FP, Hoerstrup SP. Trans-apical versus surgical implantation of autologous ovine tissue-engineered heart valves. *J. Heart Valve Dis.* 2012; 21:670–678. [PubMed: 23167234]
  7. Flanagan TC, Sachweh JS, Frese J, Schnoring H, Gronloh N, Koch S, Tolba RH, Schmitz-Rode T, Jockenhoewel S. In vivo remodeling and structural characterization of fibrin-based tissue-engineered heart valves in the adult sheep model. *Tissue engineering. Part A.* 2009; 15:2965–2976. [PubMed: 19320544]
  8. Syedain Z, Lahti MT, Johnson S, Robinson P, Ruth GR, Bianco R, Tranquillo R. Implantation of a Tissue Engineered Heart Valve from Human Fibroblasts Exhibiting Short Term Function in the Sheep Pulmonary Artery. *Cardiovascular Engineering and Technology.* 2011; 2:101–112.
  9. Dijkman PE, Driessen-Mol A, Frese L, Hoerstrup SP, Baaijens FP. Decellularized homologous tissue-engineered heart valves as off-the-shelf alternatives to xeno- and homografts. *Biomaterials.* 2012; 33:4545–4554. [PubMed: 22465337]
  10. Syedain ZH, Bradee AR, Kren S, Taylor DA, Tranquillo RT. Decellularized tissue-engineered heart valve leaflets with recellularization potential. *Tissue Eng Part A.* 2013; 19:759–769. [PubMed: 23088577]
  11. Dahl SL, Kypson AP, Lawson JH, Blum JL, Strader JT, Li Y, Manson RJ, Tente WE, DiBernardo L, Hensley MT, Carter R, Williams TP, Prichard HL, Dey MS, Begelman KG, Niklason LE. Readily available tissue-engineered vascular grafts. *Science translational medicine.* 2011; 3:68ra69.
  12. Syedain ZH, Meier L, Lahti M, Johnson S, Tranquillo RT. Implantation of Completely Biological, Aligned Engineered Arteries Pre-made from Allogeneic Fibroblasts in a Sheep Model. (Submitted 2013.)
  13. Baaijens F, Bouten C, Hoerstrup S, Mol A, Driessen N, Boerboom R. Functional tissue engineering of the aortic heart valve. *Clin. Hemorheol. Microcirc.* 2005; 33:197–199. [PubMed: 16215285]
  14. Flanagan TC, Cornelissen C, Koch S, Tschoeke B, Sachweh JS, Schmitz-Rode T, Jockenhoewel S. The in vitro development of autologous fibrin-based tissue-engineered heart valves through optimised dynamic conditioning. *Biomaterials.* 2007; 28:3388–3397. [PubMed: 17467792]
  15. Neidert MR, Tranquillo RT. Tissue-engineered valves with commissural alignment. *Tissue Eng.* 2006; 12:891–903. [PubMed: 16674301]
  16. Robinson PS, Johnson SL, Evans MC, Barocas VH, Tranquillo RT. Functional tissue-engineered valves from cell-remodeled fibrin with commissural alignment of cell-produced collagen. *Tissue engineering. Part A.* 2008; 14:83–95. [PubMed: 18333807]
  17. Cox JL, Ad N, Myers K, Gharib M, Quijano RC. Tubular heart valves: a new tissue prosthesis design—preclinical evaluation of the 3F aortic bioprosthesis. *J. Thorac. Cardiovasc. Surg.* 2005; 130:520–527. [PubMed: 16077422]
  18. Grassl ED, Oegema TR, Tranquillo RT. A fibrin-based arterial media equivalent. *Journal of biomedical materials research. Part A.* 2003; 66A:550–561. [PubMed: 12918038]
  19. Syedain ZH, Meier LA, Bjork JW, Lee A, Tranquillo RT. Implantable arterial grafts from human fibroblasts and fibrin using a multi-graft pulsed flow-stretch bioreactor with noninvasive strength monitoring. *Biomaterials.* 2011; 32:714–722. [PubMed: 20934214]
  20. Isenberg BC, Tranquillo RT. Long-term cyclic distention enhances the mechanical properties of collagen-based media-equivalents. *Ann. Biomed. Eng.* 2003; 31:937–949. [PubMed: 12918909]
  21. Syedain ZH, Weinberg JS, Tranquillo RT. Cyclic distension of fibrin-based tissue constructs: evidence of adaptation during growth of engineered connective tissue. *Proc Natl Acad Sci U S A.* 2008; 105:6537–6542. [PubMed: 18436647]
  22. Stegemann H, Stalder K. Determination of hydroxyproline. *Clin. Chim. Acta.* 1967; 18:267–273. [PubMed: 4864804]
  23. Robinson PS, Johnson SL, Evans MC, Barocas VH, Tranquillo RT. Functional tissue-engineered valves from cell-remodeled fibrin with commissural alignment of cell-produced collagen. *Tissue Eng Part A.* 2008; 14:83–95. [PubMed: 18333807]

24. Kim YJ, Sah RL, Doong JY, Grodzinsky AJ. Fluorometric assay of DNA in cartilage explants using Hoechst 33258. *Anal. Biochem.* 1988; 174:168–176. [PubMed: 2464289]
25. Tower TT, Neidert MR, Tranquillo RT. Fiber alignment imaging during mechanical testing of soft tissues. *Ann. Biomed. Eng.* 2002; 30:1221–1233. [PubMed: 12540198]
26. Nakayama Y, Yahata Y, Yamanami M, Tajikawa T, Ohba K, Kanda K, Yaku H. A completely autologous valved conduit prepared in the open form of trileaflets (type VI biovalve): mold design and valve function in vitro. *Journal of biomedical materials research. Part B, Applied biomaterials.* 2011; 99:135–141.
27. Stradins P, Lacis R, Ozolanta I, Purina B, Ose V, Feldmane L, Kasyanov V. Comparison of biomechanical and structural properties between human aortic and pulmonary valve. *Eur. J. Cardiothorac. Surg.* 2004; 26:634–639. [PubMed: 15302062]
28. Weber B, Scherman J, Emmert MY, Gruenenfelder J, Verbeek R, Bracher M, Black M, Kortsmid J, Franz T, Schoenauer R, Baumgartner L, Brokopp C, Agarkova I, Wolint P, Zund G, Falk V, Zilla P, Hoerstrup SP. Injectable living marrow stromal cell-based autologous tissue engineered heart valves: first experiences with a one-step intervention in primates. *Eur. Heart J.* 2011; 32:2830–2840. [PubMed: 21415068]
29. Williams C, Johnson SL, Robinson PS, Tranquillo RT. Cell sourcing and culture conditions for fibrin-based valve constructs. *Tissue Eng.* 2006; 12:1489–1502. [PubMed: 16846346]
30. Syedain ZH, Tranquillo RT. TGF-beta1 diminishes collagen production during long-term cyclic stretching of engineered connective tissue: implication of decreased ERK signaling. *J Biomech.* 2011; 44:848–855. [PubMed: 21251657]
31. Syedain ZH, Tranquillo RT. Controlled cyclic stretch bioreactor for tissue-engineered heart valves. *Biomaterials.* 2009; 30:4078–4084. [PubMed: 19473698]
32. Perri G, Polito A, Esposito C, Albanese SB, Francalanci P, Pongiglione G, Carotti A. Early and late failure of tissue-engineered pulmonary valve conduits used for right ventricular outflow tract reconstruction in patients with congenital heart disease. *Eur J Cardiothorac Surg.* 2012; 41:1320–1325. [PubMed: 22219487]
33. Quint C, Kondo Y, Manson RJ, Lawson JH, Dardik A, Niklason LE. Decellularized tissue-engineered blood vessel as an arterial conduit. *Proc Natl Acad Sci U S A.* 2011; 108:9214–9219. [PubMed: 21571635]
34. Gerosa G, Tarzia V, Rizzoli G, Bottio T. Small aortic annulus: the hydrodynamic performances of 5 commercially available tissue valves. *J. Thorac. Cardiovasc. Surg.* 2006; 131:1058–1064. [PubMed: 16678590]
35. Rouleau L, Tremblay D, Cartier R, Mongrain R, Leask RL. Regional variations in canine descending aortic tissue mechanical properties change with formalin fixation. *Cardiovascular pathology : the official journal of the Society for Cardiovascular Pathology.* 2012; 21:390–397. [PubMed: 22300500]
36. Christie GW. Anatomy of aortic heart valve leaflets: the influence of glutaraldehyde fixation on function. *Eur. J. Cardiothorac. Surg.* 1992; 6:S25–S32. [PubMed: 1389275]
37. Christie GW, Barratt-Boyes BG. Mechanical properties of porcine pulmonary valve leaflets: how do they differ from aortic leaflets? *Ann. Thorac. Surg.* 1995; 60:S195–S199. [PubMed: 7646158]

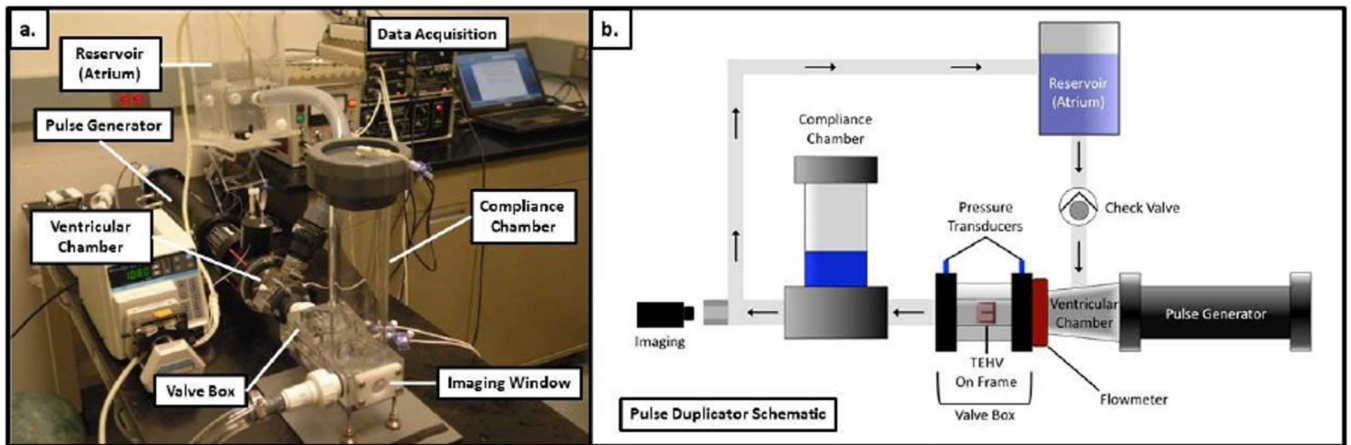


**Figure 1.** Pulse duplicator system used for testing the tubular TEHV under aortic and pulmonary conditions. A photograph of the pulse duplicator system is shown in (a) and a schematic of the key components is shown in (b). To simplify the diagram, the peristaltic pump seen in the photograph for pumping fluid from a collection chamber back to the reservoir is not included.

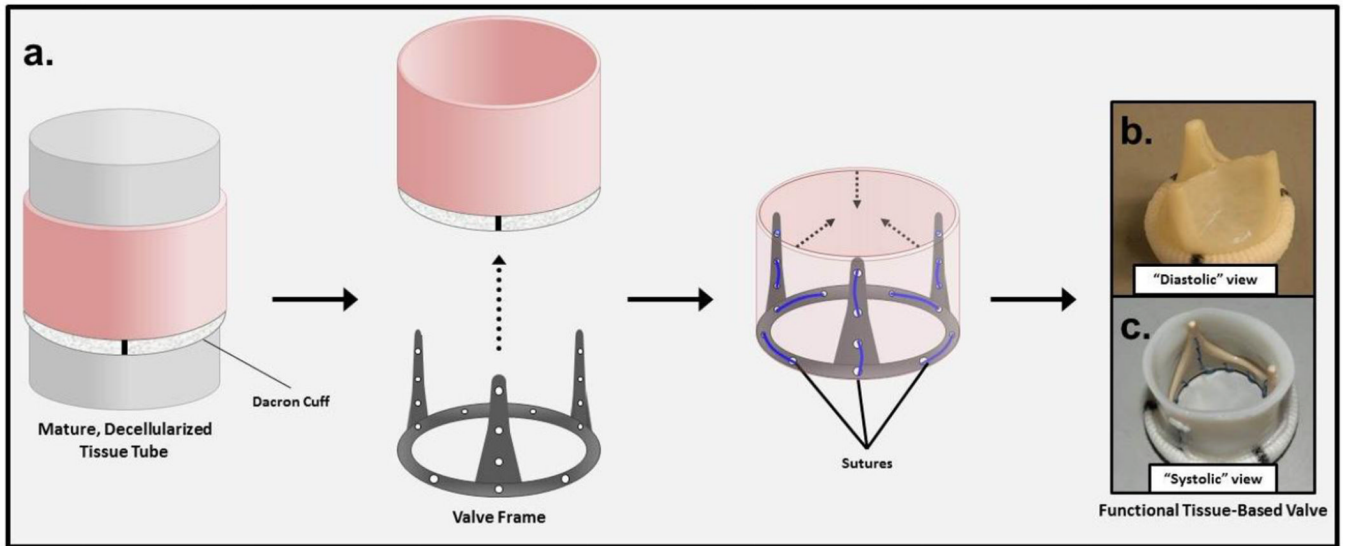


**Figure 2.** Schematic diagram of fabrication of a heart valve based on an engineered tissue tube. (a) An engineered tissue tube with a polyester cuff embedded at one end is decellularized and mounted on a custom PEEK frame using prolene suture. An image of the resulting engineered tissue tube-based valve with coapting (b) and open (c) leaflets is shown to demonstrate the valvular function of the engineered tube mounted on a custom PEEK frame.

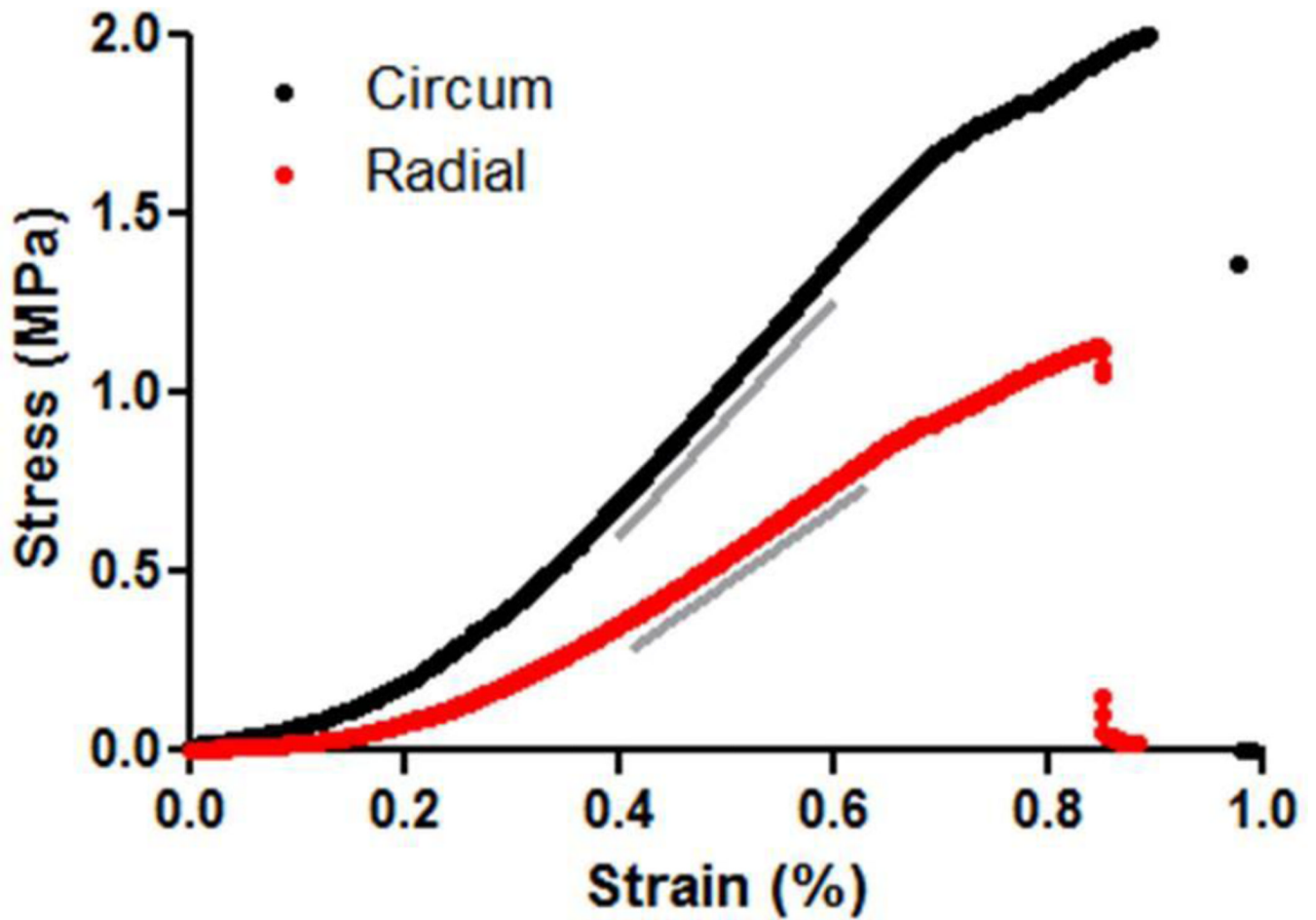


**Figure 3.** Stress-strain curves of a representative engineered tissue tube tested in tension in the circumferential (black) and radial (red) directions. Grey lines represent the regions from which the modulus was calculated.

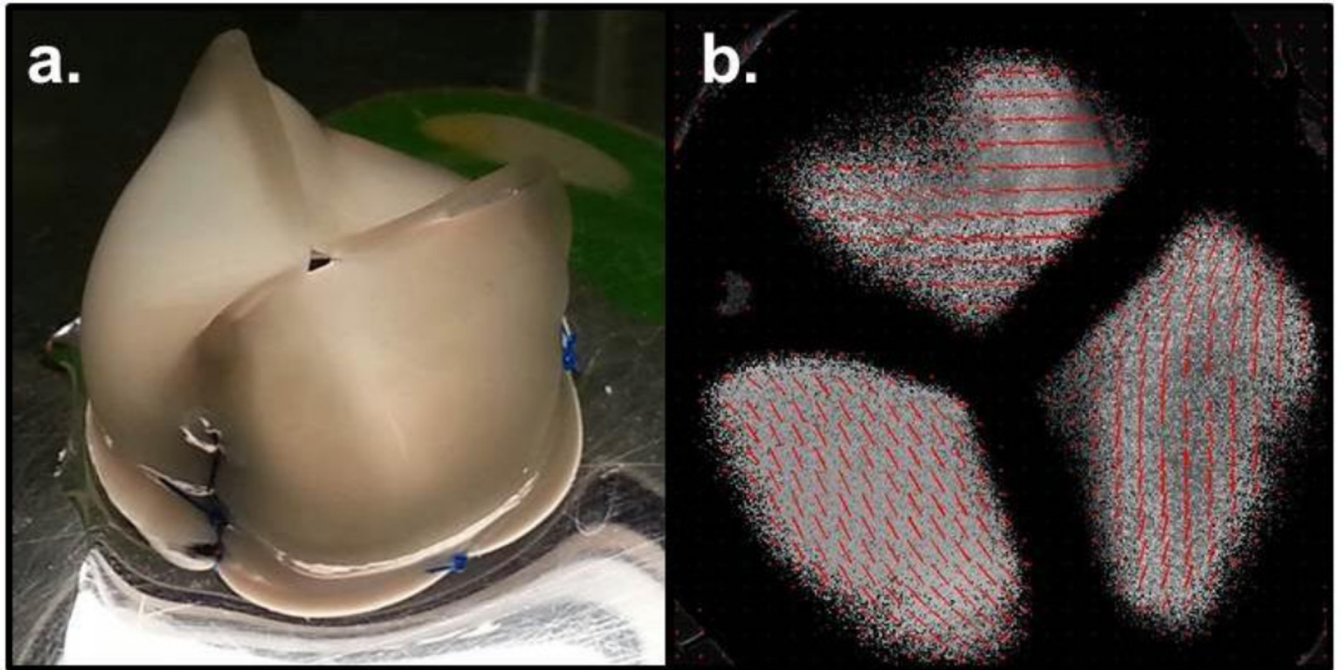


**Figure 4.** Polarized light imaging of the tubular TEHV. (a) An image of a frame-mounted valve that was used for polarized light imaging. (b) The resulting alignment map indicates underlying commissural fiber alignment present within the engineered tube valve's leaflets (red segments indicate the local average direction and strength of alignment based on polarimetry).

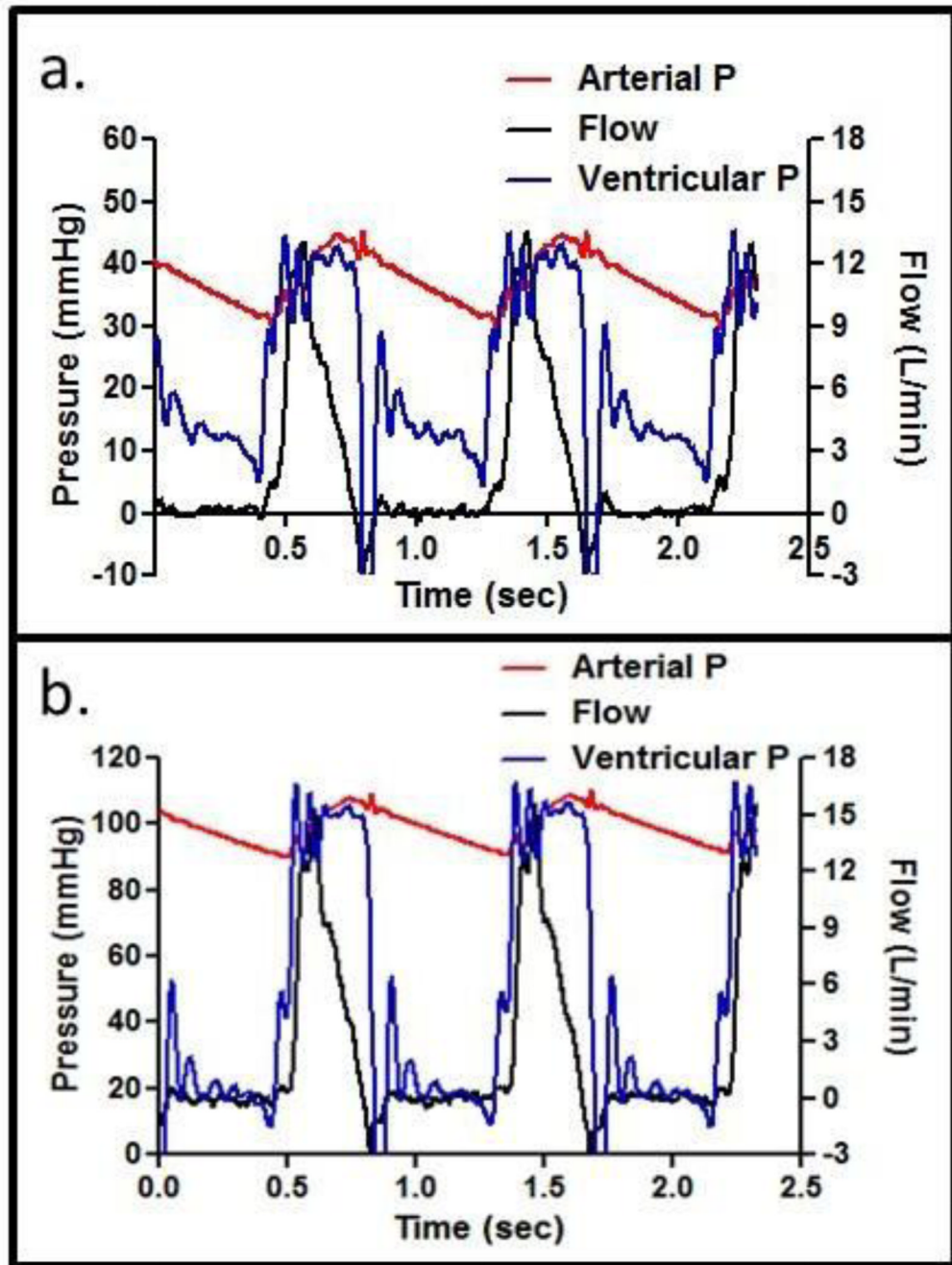


**Figure 5.** Pulse-duplicator testing of the tubular TEHV. Representative pressure-flow traces acquired under pulmonary (a) and aortic (b) conditions.

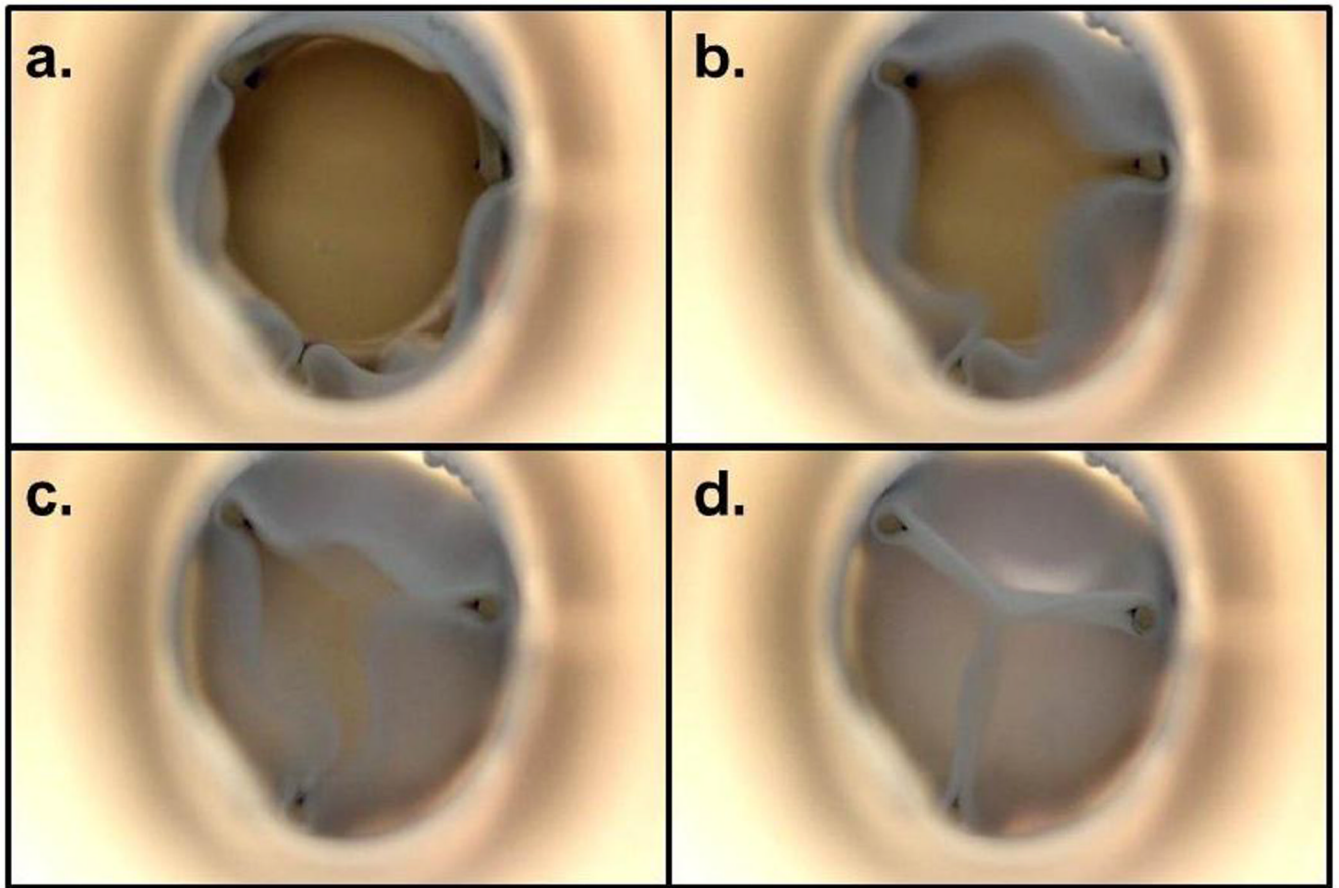


**Figure 6.** Images of the tubular TEHV undergoing testing in a pulse duplicator system. The valve orifice during peak systole is shown in (a). Following systole, the tubular TEHV “leaflets” begin to rapidly close as the downstream pressure increases (b, c). Coaptation results during diastole (d).



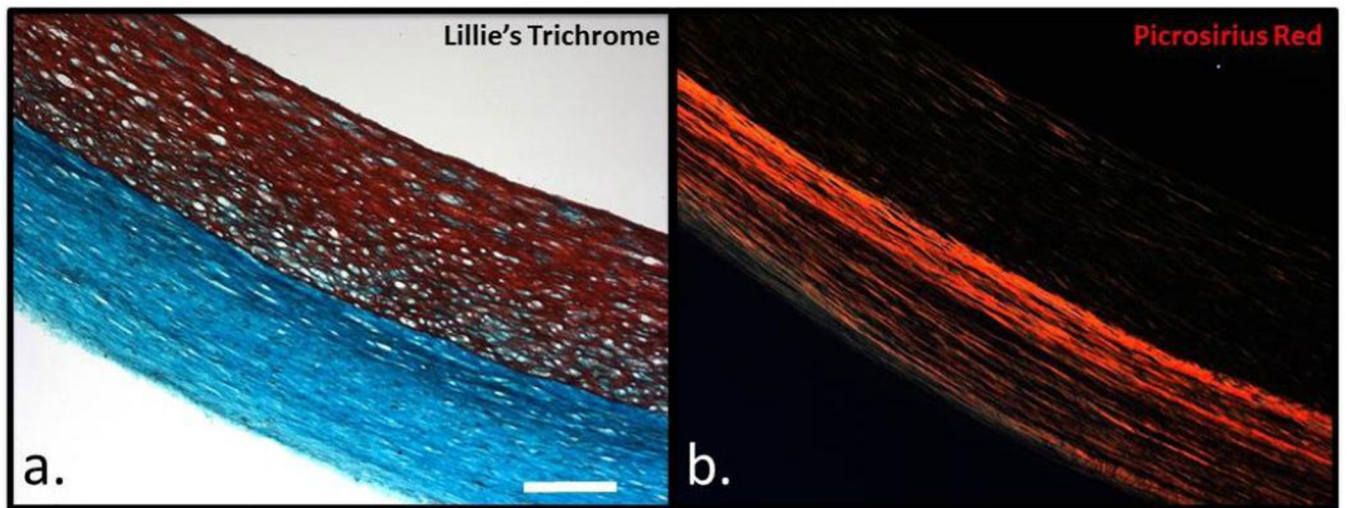


**Figure 7.** Histological analysis of engineered tissue tubes. Lillie's trichrome (a) and picrosirius red (b) staining of a decellularized 22mm ID engineered tissue tube. The scale bar in (a) is 200  $\mu$ m and applies for both images.

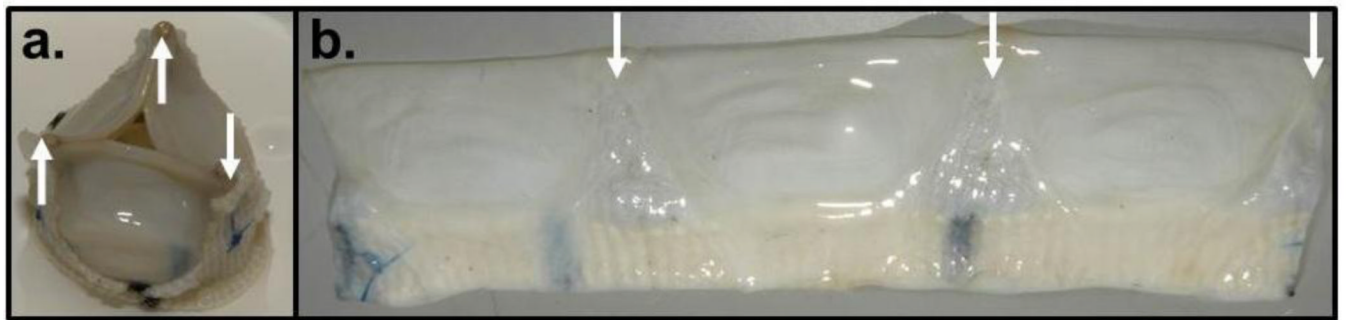


**Figure 8.** Macroscopic observations of a tubular TEHV subjected to 1M cycles in a pulse duplicator system. The valve was mounted on the custom frame (a) and fatigue-tested using the pulse duplicator system. Following fatigue testing, the tissue tube was removed and cut longitudinally for macroscopic inspection (b). The locations of the frame support struts are indicated with the white arrows in both images.

**Table 1**

Mechanical and compositional properties of the tubular TEHV

Property	Sheep PV Leaflet	Tubular TEHV
<b>Thickness</b>	0.36±0.70 mm	0.80±0.04 mm
<b>UTS (circumferential)</b>	2.03±1.70 MPa	2.74±0.66 MPa
<b>UTS (radial)</b>	0.35±0.11 MPa	0.86±0.28 MPa
<b>Modulus (circumferential)</b>	3.20±0.82 MPa	3.49±1.02 MPa
<b>Modulus (radial)</b>	1.33±0.24 MPa	1.94±0.57 MPa
<b>Strength Anisotropic Index<sup>2</sup></b>	5.80±0.83	3.20±0.24
<b>Modulus Anisotropic Index<sup>1</sup></b>	2.40±0.25	1.80±0.29
<b>Collagen Concentration</b>	54±7 mg/cm <sup>3</sup>	41±7 mg/cm <sup>3</sup>
<b>Protein Concentration</b>	83±2 mg/cm <sup>3</sup>	78±17 mg/cm <sup>3</sup>
<b>DNA Content</b>	96±8 million cells/cm <sup>3</sup>	3±1 million cells/ cm <sup>3</sup>

<sup>1</sup>. Modulus Anisotropic Index is defined as the ratio of modulus in circumferential to radial direction.

<sup>2</sup>. Strength Anisotropic Index is defined as the ratio of UTS in circumferential to radial direction.

**Table 2**

Pulse Duplicator Testing of the Tubular TEHV

	<b>Pulmonary conditions</b>	<b>Aortic conditions</b>
<b>Systolic P</b>	0.7±0.5 mmHg	2.7±1.0 mmHg
<b>Diastolic P</b>	11.1±2.7 mmHg	100±15 mmHg
<b>Average Flow Rate</b>	5.1±1.5 LPM	5.5±1.0 LPM
<b>Peak Flow Rate</b>	10.9±0.1 LPM	12.7±1.4 LPM
<b>EOA<sup>I</sup> (%)</b>	95±1 %	96±2 %
<b>Regurgitant Fraction</b>	4.1±3.8 %	5.1±4.5 %

<sup>I</sup>. Effective orifice area (EOA) percentage is with respect to a circular orifice with radius equal to the frame inner diameter (19mm).